

Vanadyl *tert*-Butoxy Orthosilicate, OV[OSi(O^tBu)₃]₃: A Model for Isolated Vanadyl Sites on Silica and a Precursor to Vanadia–Silica Xerogels[†]

Ron Rulkens,^{‡,§} Jonathan L. Male,^{‡,§} Karl W. Terry,[†] Bryan Olthof,^{§,||} Andrei Khodakov,^{§,||} Alexis T. Bell,^{§,||} Enrique Iglesia,^{§,||} and T. Don Tilley^{*,‡,§}

Department of Chemistry and the Department of Chemical Engineering, University of California, Berkeley, Berkeley, California 94720-1460, and the Chemical and Materials Science Divisions, Lawrence Berkeley National Laboratory, 1 Cyclotron Road, Berkeley, California 94720

Received June 3, 1999. Revised Manuscript Received July 29, 1999

The single source precursor OV[OSi(O^tBu)₃]₃ was synthesized in high yield from OVCl₃ and HOSi(O^tBu)₃. This tri(alkoxy)siloxy complex was characterized by ¹H, ¹³C, ²⁹Si, and ⁵¹V NMR, FT-Raman, FT-IR, EXAFS, and UV–vis spectroscopies and by mass spectrometry. In the Raman spectrum of OV[OSi(O^tBu)₃]₃, V=O (1038 cm⁻¹) and V–O (651, 674, and 705 cm⁻¹) vibrations were observed. The ⁵¹V NMR shift was observed at –777 ppm and the ²⁹Si NMR resonance appears at –98 ppm. Thermolysis in *n*-octane at 180 °C resulted in formation of a green gel which upon drying in air formed a xerogel with a surface area of 320 m² g⁻¹, an average pore size of 140 Å, and a total pore volume of 2.25 cm³ g⁻¹. The calcined xerogel is similar to bulk V₂O₅ in catalytic performance for propane oxidative dehydrogenation.

Introduction

The direct oxidation of organic compounds with molecular oxygen is typically nonselective and often leads to C–C bond cleavage or complete combustion. For this reason, studies on the selective oxidation of hydrocarbons have focused on metal oxide catalysts, which can provide alternative (and more selective) oxidation pathways. The high oxidation potential for vanadium(V) oxide and the ease with which vanadium can shuttle between the +5, +4, and +3 oxidation states make vanadium a popular element of choice for the active component in heterogeneous oxidation catalysts.¹ For example, vanadia–silica catalyzes selective oxidations of light hydrocarbons at low vanadium loadings.^{2,3} The most ordered vanadia–silica systems include zeolitic materials such as vanadium–silicalite, in which a small percentage of the silicon is substituted by vanadium,^{4–9}

and vanadium-containing mesoporous materials.^{10–12} Hydrolytic (sol–gel type) methods have been used to produce amorphous, vanadia-containing silica aerogels and xerogels.^{13–17} In addition, vanadia–silica catalysts have been prepared by treating commercially available silica with a variety of vanadia sources, followed by a calcination step.^{9,18–24}

In general, vanadia–silica catalysts have proven difficult to characterize. In some cases, this results from the relatively low vanadium content in the material and/or its presence in many forms (coordination environments, oxidation states, etc.). Nonetheless, many studies have addressed the nature of the active single-site vanadium species (**1**) present in these materials, and a

[‡] Department of Chemistry, University of California, Berkeley.

[§] Lawrence Berkeley National Laboratory.

[†] Part of this work is contained in the Ph.D. thesis of K.W.T., University of California, San Diego, 1993.

^{||} Department of Chemical Engineering, University of California, Berkeley.

(1) Albonetti, S.; Cavani, F.; Trifirò, F. *Catal. Rev. Sci. Eng.* **1996**, *38*, 413.

(2) Centi, G.; Trifiro, F. *Appl. Catal. A* **1996**, *143*, 3.

(3) Mamedov, E. A.; Corberán, C. *Appl. Catal. A* **1995**, *127*, 1 and references therein.

(4) Centi, G.; Perathoner, S.; Trifirò, F.; Aboukais, A.; Aissi, C. F.; Guelton, M. *J. Phys. Chem.* **1992**, *96*, 2617.

(5) Kornatowski, J.; Wichterlová, B.; Jirkovský, J.; Löffler, E.; Pilz, W. *J. Chem. Soc., Faraday Trans.* **1996**, *92*, 1067.

(6) Sen, T.; Rajamohanam, P. R.; Ganapathy, S.; Sivasankar, S. *J. Catal.* **1996**, *163*, 354.

(7) Rocha, J.; Brandao, P.; Lin, Z.; Anderson, M. W.; Alfredsson, V.; Terasaki, O. *Angew. Chem., Int. Ed. Engl.* **1996**, *36*, 100.

(8) Reddy, K. M.; Moudrakovski, I.; Sayari, A. *J. Chem. Soc., Chem. Commun.* **1994**, 1491.

(9) Wang, C. B.; Deo, G.; Wachs, I. E. *J. Catal.* **1998**, *178*, 640.

(10) Reddy, K. M.; Moudrakovski, I.; Sayari, A. *J. Chem. Soc., Chem. Commun.* **1994**, 1059.

(11) Morey, M.; Davidson, A.; Eckert, H.; Stucky, G. *Chem. Mater.* **1996**, *8*, 486.

(12) Luca, V.; MacLachlan, D. J.; Morgan, K. *Chem. Mater.* **1997**, *9*, 2720.

(13) Dutoit, D. C. M.; Schneider, M.; Fabrizioli, P.; Baiker, A. *Chem. Mater.* **1996**, *8*, 734.

(14) Dutoit, D. C. M.; Schneider, M.; Fabrizioli, P.; Baiker, A. *J. Chem. Mater.* **1997**, *7*, 271.

(15) Neumann, R.; Levin-Elad, M. *Appl. Catal.* **1995**, *122*, 85.

(16) Stiegman, A. E.; Eckert, H.; Plett, G.; Kim, S. S.; Anderson, M.; Yavrouian, A. *Chem. Mater.* **1993**, *5*, 1591.

(17) Owens, L.; Kung, H. H. *J. Catal.* **1993**, *144*, 202.

(18) Schraml-Marth, M.; Wokaun, A.; Pohl, M.; Krauss, H.-L. *J. Chem. Soc., Faraday Trans.* **1991**, *87*, 2635.

(19) Deo, G.; Wachs, I. E. *J. Catal.* **1994**, *146*, 323.

(20) Haber, J.; Kozłowska, A.; Kozłowski, R. *J. Catal.* **1986**, *102*, 52.

(21) van Hengstum, A. J.; van Ommen, J. G.; Bosch, H.; Gellings, P. *J. Appl. Catal.* **1983**, *5*, 207.

(22) Kijenski, J.; Baiker, A.; Glinski, M.; Dollenmeier, P.; Wokaun, A. *J. Catal.* **1986**, *101*, 1.

(23) van der Voort, P.; Possemiers, K.; Vansant, E. F. *J. Chem. Soc., Faraday Trans.* **1996**, *92*, 843.

(24) Inumaru, K.; Misono, M.; Okuhara, T. *Appl. Catal. A* **1997**, *149*, 133.

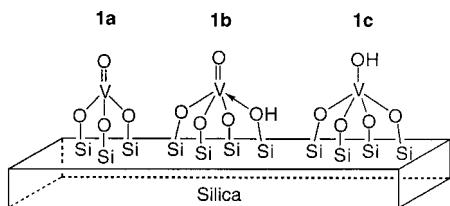
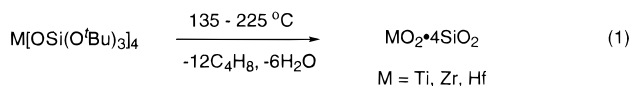


Figure 1. Proposed geometries of isolated vanadium species on a silica surface.

variety of structures have been proposed (see Figure 1).^{18,23,24} Particular attention has been focused on a tripodally anchored V=O group (**1a**), which is the most favored structure attributed to isolated vanadia centers,²⁵ but five-coordinate structures (**1b** and **1c**) have also been proposed.^{4–6} Clearly, molecular model compounds in which the chemical composition and coordination sphere closely resemble those present in **1a** would offer valuable comparative data. Vanadium–silicon molecular model compounds studied previously in this context are [Ph₃SiO]₃VO (**2**)^{26,27} and (*c*-C₆H₁₁)₇-(Si₇O₁₂)VO (**3**),²⁶ which exists in equilibrium with its dimer (**4**).^{26,28} Although these molecular species represent interesting structural models for isolated vanadyl sites on silica, the presence of the organic substituents on silicon has complicated the direct comparison of spectroscopic data with vanadia–silica catalysts. Also, with respect to development of molecular routes to well-defined structures, the silicon–carbon bonds in **2–4** make these molecules unsuitable as direct precursors to vanadia–silica materials.

In general, a challenging aspect of the synthesis of tailored vanadia–silica catalysts is the development of methods for the homogeneous incorporation of vanadium into the structure, particularly at high vanadium loadings. Such high dispersions are difficult to achieve by traditional wet impregnation methods, because crystalline V₂O₅ domains tend to form under aqueous conditions.^{3,24,29} An attractive alternative approach is suggested by the single-source precursor route to mixed-element oxides, which has been employed by our group in the synthesis of a number of highly dispersed metal oxide–silica materials.^{30–34} For example, the group 4 tri(alkoxy)siloxy complexes M[OSi(O*t*Bu)₃]₄ (M = Ti, Zr, Hf) convert readily to MO₂·4SiO₂ materials with very high surface areas, at temperatures as low as 135 °C (eq 1).^{30,31}



(25) Tran, K.; Hanning-Lee, M. A.; Biswas, A.; Stiegmann, A. E.; Scott, G. W. *J. Am. Chem. Soc.* **1995**, *117*, 2618.

(26) Feher, F. J.; Walzer, J. F. *Inorg. Chem.* **1991**, *30*, 1689.

(27) Huang, M.; DeKock, C. W. *Inorg. Chem.* **1993**, *32*, 2287.

(28) Das, N.; Eckert, H.; Hu, H.; Wachs, I. E.; Walzer, J. F.; Feher, F. J. *J. Phys. Chem.* **1993**, *97*, 8240.

(29) van der Voort, P.; White, M. G.; Mitchell, M. B.; Verberckmoes, A. A.; Vansant, E. F. *Spectrochim. Acta A* **1997**, *53*, 2181.

(30) Terry, K. W.; Tilley, T. D. *Chem. Mater.* **1991**, *3*, 1001.

(31) Terry, K. W.; Lugmair, C. G.; Tilley, T. D. *J. Am. Chem. Soc.* **1997**, *119*, 9745.

(32) Terry, K. W.; Lugmair, C. G.; Gantzel, P. K.; Tilley, T. D. *Chem. Mater.* **1996**, *8*, 274.

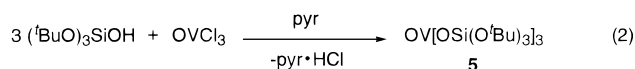
(33) McMullen, A. K.; Tilley, T. D.; Rheingold, A. L.; Geib, S. J. *Inorg. Chem.* **1990**, *29*, 2228.

(34) Su, K.; Tilley, T. D. *Chem. Mater.* **1997**, *9*, 588.

As part of this effort, our research has focused on the synthesis of molecular single-source precursors to vanadia–silica catalysts. For this purpose, we have synthesized OV[OSi(O*t*Bu)₃]₃ (**5**)³⁵ and have recently reported its cothermolysis with Zr(OCMe₂Et)₄ in organic solvents to produce mesoporous catalysts for the oxidative dehydrogenation (ODH) of propane.^{36,37} In related work, Neumann and co-workers have recently obtained a vanadia–silica material via the presumed generation of **5** (not isolated or characterized) in solution, followed by removal of solvent and calcination of the residue at 250 °C.³⁸ In this paper, we present details on the synthesis and characterization of compound **5**, which serves as a useful model for surface sites of type **1a**. In addition, we have used the isolated compound as a single-source precursor for the synthesis of a highly porous vanadia–silica xerogel, which has been evaluated as a catalyst for the ODH of propane.

Results and Discussion

Synthesis and Characterization of 5. The reaction of OVCl₃ with 3 equiv of (*t*BuO)₃SiOH in the presence of pyridine gives **5** as a white opaque solid in 85% yield after crystallization from dichloromethane (eq 2).³⁷ This compound is very soluble in nonpolar hydrocarbons, and hydrolyzes slowly in air.



The UV–vis spectrum of **5** in hexane contains a broad absorption band at 250 nm ($\epsilon = 9.8 \times 10^3 \text{ M}^{-1} \text{ cm}^{-1}$), assigned to an O → V ligand-to-metal charge-transfer (LMCT) band. For isolated O₃V=O sites on silica, λ_{max} values of <350 nm have generally been reported.¹¹ For example, materials prepared by anchoring vanadyl groups onto MCM-48 silica were proposed to contain pseudotetrahedral O₃V=O centers of type **1a**, giving rise to broad absorptions at 325 ± 10 nm.¹¹ The spectroscopic properties of **1a** were also investigated for discrete vanadyl centers (0.005% mol vanadium) dispersed in a silica xerogel matrix.^{16,25,39} For these materials, LMCT transitions observed at room temperature as unresolved absorption shoulders at 235 nm ($\epsilon = 5.2 \times 10^3 \text{ M}^{-1} \text{ cm}^{-1}$) and 330 nm ($\epsilon = 5.0 \times 10^2 \text{ M}^{-1} \text{ cm}^{-1}$) were resolved into spectral features at 240, 290, and 323 nm, at 14 K.^{25,39} Stiegman and Scott characterized the lowest energy band as involving promotion of an electron from an orbital based on the Si-bonded oxygens to the metal center and not, as previously assumed, a transition involving only the V=O group. The other two bands were assigned as $\pi \rightarrow \pi^*$ V=O transitions.^{25,39} Our observation of only one charge-transfer band, with a similar molar absorptivity as the most intense OV(OSi)₃ chromophore of **1a** (as prepared by Stiegman and Scott), suggests that assignments for such bands in vanadia–

(35) Terry, K. W. Ph.D. Thesis, UC San Diego, 1993.

(36) Rulkens, R.; Terry, K. W.; Tilley, T. D. In *215th ACS National Meeting*; American Chemical Society, Dallas, TX, 1998; CATL 018 (part 2).

(37) Rulkens, R.; Tilley, T. D. *J. Am. Chem. Soc.* **1998**, *120*, 9959.

(38) Juwiler, D.; Blum, J.; Neumann, R. *Chem. Commun.* **1998**, 1123.

(39) Tran, K.; Stiegman, A. E.; Scott, G. W. *Inorg. Chim. Acta* **1996**, *243*, 185.

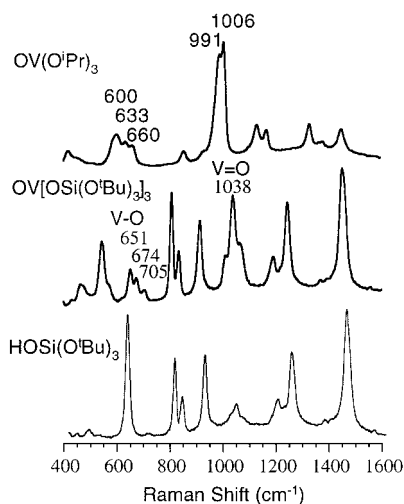


Figure 2. Raman spectra of HOSi(O'Bu)₃, OV[OSi(O'Bu)₃]₃ (**5**), and OV(O'Pr)₃.

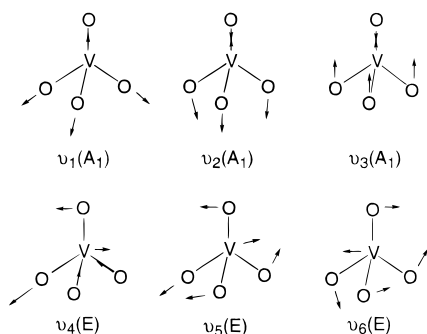


Figure 3. The six normal vibrational modes for the O=V(-O)₃ group.^{43,44}

silica materials may not be as straightforward as previously believed.⁴⁰

It was of interest to examine the Raman spectrum of **5**, since its OV(OSiO₃)₃ core would seem to provide an excellent model for isolated vanadyl groups on silica. Previously, compounds **2** and **4** were studied in this context, but bands for the V=O and V-O-Si groups were obscured by intense bands for the hydrocarbon portions of these molecules.²⁸ Assignments of the bands for **5** were aided by comparisons with Raman spectra for HOSi(O'Bu)₃ and OV(O'Pr)₃ (Figure 2) and by previous assignments for the spectrum of OV(O'Pr)₃.^{41,42} Most apparent in the Raman spectrum of **5** is the intense band at 1038 cm⁻¹, which can be assigned to the ν₃ mode of a O=VO₃ moiety (Figure 3).^{43,44} This assignment is also consistent with those for simple molecules such as OVX₃ (X = F, Cl, Br)⁴⁵⁻⁴⁷ and OV-

(OR)₃ (R = ^tPr, ^tBu).⁴¹ Less intense bands at 1066 and 1010 cm⁻¹ may be due to a C-O-Si stretching oscillation^{44,48} and an asymmetric O-Si-O vibrational mode, respectively.^{44,49,50} The related bands in HOSi(O'Bu)₃ appear to be those observed at 1032 and 1014 cm⁻¹ (Figure 2). Note, however, that one of these bands may also correspond to a CH₃ wagging mode.⁴¹ Pairs of bands at 914 and 545 cm⁻¹ (in **5**) and 915 and 623 cm⁻¹ (in HOSi(O'Bu)₃) are assigned as Si-O stretching vibrations.^{44,48,50}

Comparisons of the Raman spectra of **5** and OV(Oⁱ-Pr)₃ reveal striking similarities in the V-O stretching regions, with the latter alkoxide complex exhibiting bands at lower frequencies (by 41–51 cm⁻¹). Bands in the Raman spectrum of **5** at 651, 674, and 705 cm⁻¹, which do not appear in the spectrum of HOSi(O'Bu)₃ (Figure 2), are assigned to stretching and bending modes involving the V-O bonds. On the basis of comparisons with the Raman spectra of OVCl₃, OVf₃, and OV(O'Pr)₃, the band at 651 cm⁻¹ is assigned to a ν₁ mode and the bands at 674 and 705 cm⁻¹ to ν₄ and 2ν₅ modes (Figure 3).^{41,43-47} In addition, V-O-Si vibrational modes at ca. 910–970 cm⁻¹ were not observed, as they are in the infrared spectrum (see below), perhaps because the ionic character of these linkages render them Raman-inactive.^{25,28}

For catalytic systems with surface species of type **1**, relatively intense, sharp bands in the Raman spectra at 1035–1042 cm⁻¹ have been assigned to V=O oscillations.^{14,24,28,51,52} The identity of this band has also been confirmed by ¹⁸O labeling.⁵¹ Recently, an in situ Raman study of a 5% V₂O₅/SiO₂ material during methanol oxidation revealed three Raman bands at 1069, 1029, and 665 cm⁻¹, which were assigned to C-O, V=O, and V-O vibrations, respectively, for surface-bound (Si-O)_{3-n}V(O)(OCH₃)_n (n = 1 or 2).⁵³ These assignments are in agreement with those made for the molecular complex **5**.

Hardcastle and Wachs previously compared Raman spectra for a series of reference vanadium compounds, and they correlated the bond order and VO bond length with Raman stretching frequencies.⁵⁴ On the basis of these correlations, the VO bond lengths and bond orders for **5** are 1.58 ± 0.02 Å and 1.91, respectively, for the V=O bond, and 1.82 ± 0.02 Å and 0.92 for the V-O single bonds. For comparison, the V=O bond lengths for compounds **2** and **4** are 1.572(2) and 1.564(8) Å,²⁶ respectively; thus they are identical to the V=O bond length for **5** derived from its 1038 cm⁻¹ Raman band (within estimated standard deviations). The average

(40) Also see: Luan, Z.; Xu, J.; He, H.; Klinowski, J.; Kevan, L. *J. Phys. Chem.* **1996**, *100*, 19595.

(41) Witke, Von K.; Lachawicz, A.; Brüser, W.; Zeigan, D. *Z. Anorg. Allg. Chem.* **1980**, *465*, 193.

(42) Assignment of the Raman spectrum of OV(O'Pr)₃ (ref 41): 1451 (δ(CH₃ asym), 1380 (δ(CH₃) sym), 1330 (δ(C-H)), 1167 (δ(CH₃) wagging), 1132 (ν(C-C₂), ν(C-O)), 1005 and 991 (ν(V=O)), 854 (δ-(CH₃) wagging), 660 and 634 (ν(VO)₃ asym), 602 (ν(VO)₃ sym), 446 (δ(C-C-C)), 417 and 332 (δ(C-C-O)), 215 (δ(VO)₃ sym), 180 (VO)₃ rocking) cm⁻¹. The authors suggest that OV(O'Pr)₃ exists as an equilibrium mixture of three rotomers, such that more than one V=O stretch is observed.

(43) Herzberg, G. In *Molecular Spectra and Molecular Structure*; D. van Nostrand Company, Inc.: New York, 1945; p 306.

(44) Nakamoto, K. *Infrared and Raman Spectra of Inorganic and Coordination Compounds: Part A: Theory and Applications in Inorganic Chemistry*, 5th ed.; Wiley-Interscience: New York, 1997.

(45) Selig, H.; Claassen, H. H. *J. Chem. Phys.* **1966**, *44*, 1404.

(46) Miller, F. A.; Cousins, L. R. *J. Chem. Phys.* **1957**, *26*, 329.

(47) Miller, F. A.; Baer, W. K. *Spectrochim. Acta* **1961**, *17*, 112.

(48) Barraclough, C. G.; Bradley, D. C.; Lewis, J.; Thomas, I. M. *J. Chem. Soc.* **1961**, 2601.

(49) Kornatowski, J.; Sychev, M.; Kuzenkov, S.; Strnadová, K.; Pilz, W.; Kassner, D.; Pieper, G.; Baur, H. *J. Chem. Soc., Faraday Trans.* **1995**, *91*, 2217.

(50) A geometry optimization of HOSi(O'Bu)₃ and a subsequent frequency analysis using MacSpartan is also consistent with this assignment.

(51) Oyama, T.; Went, G. T.; Lewis, K. B.; Bell, A. T.; Somorjai, G. A. *J. Phys. Chem.* **1989**, *93*, 6786.

(52) Went, G. T.; Oyama, S. T.; Bell, A. T. *J. Phys. Chem.* **1990**, *94*, 4240.

(53) Gao, X.; Bare, S. R.; Weckhuysen, B. M.; Wachs, I. E. *J. Phys. Chem.* **1998**, *102*, 10842.

(54) Hardcastle, F. D.; Wachs, I. E. *J. Phys. Chem.* **1991**, *95*, 5031.

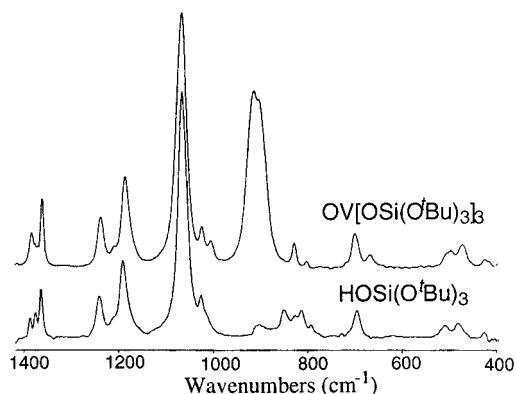


Figure 4. Infrared spectra of $\text{HOSi}(\text{O}^t\text{-Bu})_3$ and $\text{OV}[\text{OSi}(\text{O}^t\text{-Bu})_3]_3$ (**5**).

V–O single bond lengths in **2** and **4** are 1.742 and 1.752 Å, respectively, and thus shorter (by 0.07–0.08 Å) than the V–O bond length derived from the Raman band of **5** at 651 cm^{-1} . A V–O bond length of ca. 1.72 Å was estimated for **1a** from generalized valence bond calculations.²⁵

The infrared spectra of **5** and $\text{HOSi}(\text{O}^t\text{-Bu})_3$ (in hexane, at equivalent concentrations of $\text{OSi}(\text{O}^t\text{-Bu})_3$ groups) are compared in Figure 4. The most intense peak in both spectra is assigned as the Si–O–C stretching band at ca. 1070 cm^{-1} , which compares well to the assignment made for this band in the Raman spectrum of **5** (1066 cm^{-1}).^{44,55} Many bands in the IR spectrum of **5** can be assigned to the $(^t\text{BuO})_3\text{SiO}$ ligands, but two equally intense overlapping bands at 910 and 920 cm^{-1} are unique to the IR spectrum of **5**. We assign both vibrations to the Si–O–V linkage.^{56,57} The analogous vibrations for sites of type **1** are usually assigned to a single band at ca. $928\text{--}937\text{ cm}^{-1}$, overlapping with a silica Si–OH band at 960 cm^{-1} .^{12,14,16,25,49} The true assignments of these bands are crucial because deconvolution of the broad band observed at ca. 950 cm^{-1} is used to provide indications of the dispersity of vanadia in silica.^{12,14} From the spectra of Figure 4, it seems that the broadness of IR bands typically assigned to Si–O–V linkages of vanadia–silica materials can also be explained by the presence of two overlapping bands arising solely from Si–O–V vibrations, rather than from overlapping Si–O–V and Si–O–H bands. In support of this, Figure 4 shows that the intensity of the Si–O–H bending vibration (905 cm^{-1}) in the spectrum of $\text{HOSi}(\text{O}^t\text{-Bu})_3$ is relatively small compared to that of the Si–O–V vibrations ($910, 920\text{ cm}^{-1}$) in the spectrum of **5**. For this reason we believe that the Si–O–H band may not significantly contribute to convolution of a broad band observed at ca. 950 cm^{-1} for vanadia–silica materials dominated by vanadium environments of type **1a**, with very low concentrations of SiOH sites. On the basis of comparisons with the Raman spectrum of **5**, a small band at 672 cm^{-1} (in the IR spectrum) should probably be assigned to a ν_4 or $2\nu_5$ vibrational mode for the OVO_3 core (Figure 3), which according to symmetry rules is both IR and Raman active (674 cm^{-1} , Figure 2).^{41,43–47} Two small peaks (at 1029 and 1010 cm^{-1})

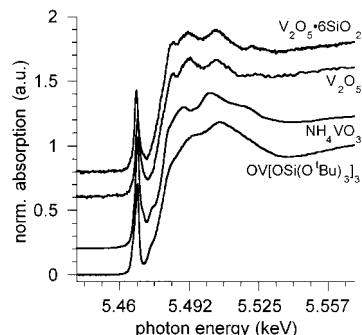


Figure 5. The near-edge EXAFS spectra of selected vanadium compounds and **5**.

appear in the region expected for the V=O stretch (ν_3 mode, Figure 3). The peak at 1029 cm^{-1} would correspond most closely to the one assigned to this stretch in the Raman spectrum (at 1038 cm^{-1}).^{12,45–47,56–59} The band at 1010 cm^{-1} (also observed in the Raman spectrum) is probably due to an O–Si–O vibration.^{44,50}

Repeated attempts to obtain a single crystal of **5** suitable for crystallographic X-ray analysis were unsuccessful. Therefore, the local molecular structure of **5** was examined by X-ray absorption spectroscopy. The vanadium K-edge absorption spectrum was recorded for $\text{OV}[\text{OSi}(\text{O}^t\text{-Bu})_3]_3$ and compared to those for NH_4VO_3 and V_2O_5 (compounds with known structures).^{60–62} It has been shown in the literature that both near-edge absorption spectra and EXAFS can provide information on the local coordination of vanadium in its compounds.^{24,63,64} The near-edge spectrum of the complex $\text{OV}[\text{OSi}(\text{O}^t\text{-Bu})_3]_3$ resembles that of NH_4VO_3 , which is often used as a V(+5) standard with tetrahedral coordination (Figure 5). These data therefore support a distorted tetrahedral coordination in $\text{OV}[\text{OSi}(\text{O}^t\text{-Bu})_3]_3$.

The fine structure extracted from X-ray absorption spectra for all compounds studied were transformed from k space (k weighting 3, 1.88–12.86 borders in k space, Hanning function, Å^{-1}) to R space in order to obtain the radial distribution function (RDF). The peaks in the RDF are usually attributed to different coordination spheres around the vanadium absorber.⁶⁵ The RDF of $\text{OV}[\text{OSi}(\text{O}^t\text{-Bu})_3]_3$ resembles that of NH_4VO_3 and contains two peaks at the two different V–O bond lengths expected in tetrahedral V^{+5} compounds. The contribution to the fine structure coming from V–O coordination shells was isolated by inverse Fourier transform of the RDF over the 0.85–2.30 Å region and fitted using single scattering analysis methods.^{66,67} The phase and amplitude of the V–O coordination were

(58) Huuhtanen, J.; Sanati, M.; Andersson, A.; Andersson, S. L. T. *Appl. Catal. A* **1993**, *97*, 197.

(59) Sekiguchi, S.; Kurihara, A. *Bull. Chem. Soc. Jpn.* **1969**, *42*, 1453.

(60) Wong, J.; Lytle, F. W.; Messmer, R. P.; Maylotte, D. H. *Phys. Rev. B* **1984**, *30*, 5596.

(61) Evans, H. T., Jr. *Z. Kristallogr. Kristallgeom. Kristallphys. Kristallchem.* **1960**, *114*, 257.

(62) Byström, A.; Willhelmi, K.-A.; Brotzen, O. *Acta Chem. Scand.* **1950**, *4*, 1119.

(63) Yoshida, S.; Tanaka, T.; Nishimura, Y.; Mizutani, H.; Funabiki, T. In *Proceedings of the 9th International Congress on Catalysis*, Calgary, Canada, 1988, Vol. 3, 1473.

(64) Zhang, S. G.; Higashimoto, S.; Yamashita, H.; Anpo, M. *J. Phys. Chem. B* **1998**, *102*, 5590.

(65) *X-ray Absorption: Principles, Applications, Techniques of EXAFS, SEXAFS and XANES*; Koningsberger, D. C., Prins, R., Eds., Wiley-Interscience: New York, 1988.

(55) Zeitler, V. A.; Brown, C. A. *J. Phys. Chem.* **1957**, *61*, 1174.

(56) Rice, G. L.; Scott, S. L. *Langmuir* **1997**, *13*, 1545.

(57) Rice, G. L.; Scott, S. L. *J. Mol. Cat. A: Chem.* **1997**, *125*, 73.

We thank a reviewer for pointing out this reference.

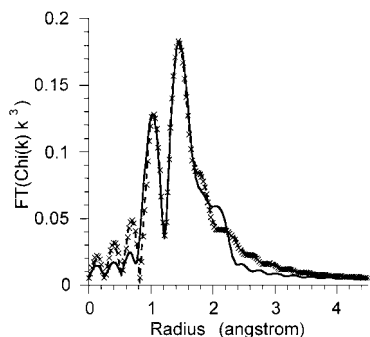


Figure 6. The radial distribution functions derived from the simulated EXAFS spectra of **2** (x) and **4** (---), fit to the radial distribution functions of **5** obtained from an experimental EXAFS spectrum (—).

calculated ab initio using the FEFF7 code and the atomic coordinates from the molecular structures of the complexes $(\text{Ph}_3\text{SiO})_3\text{VO}$ (**2**)^{26,27} and $[(c\text{-C}_6\text{H}_{11})_7(\text{Si}_7\text{O}_{12})\text{VO}]_2$ (**4**).^{26,66–69}

The simulated EXAFS were fit to the filtered experimental spectra of $\text{OV}[\text{OSi}(\text{O}^t\text{Bu})_3]$ (Figure 6). The $\text{V}=\text{O}$ and $\text{V}-\text{O}$ bond lengths were found to be longer in **5** (1.596 and 1.770 Å, respectively) than in **2** ($\text{V}=\text{O}$, 1.572(2) Å; $\text{V}-\text{O}$, 1.74 Å, average) and **4** ($\text{V}=\text{O}$, 1.564(8) Å; $\text{V}-\text{O}$, 1.75 Å, average).^{26,27} This is consistent with the trends in bond lengths predicted from the Raman spectra.

The solution ^{51}V NMR spectrum of **5** consists of a single, very sharp signal at -777 ppm ($\omega_{1/2} = 65$ Hz). This chemical shift is at relatively high field compared to those assigned to 4-coordinate vanadium atoms in **1** (for which various values such as -560 ,⁵ -605 ,¹² and -710 ± 10 ppm²⁸ have been reported), **2** (-725 ppm),²⁶ **3** (-676 ppm, $\omega_{1/2} = 510$ Hz),²⁶ and **4** (-710 ppm, $\omega_{1/2} = 430$ Hz).²⁶ For structurally similar monomeric orthovanadates (M_3VO_4), chemical shifts are observed to move to higher fields as the $\text{V}-\text{O}$ bond length of the salts is increased.⁴ Thus, for Ti_3VO_4 , $d(\text{V}-\text{O}) = 1.61\text{--}1.62$ Å and $\delta = -480$ ppm and for K_3VO_4 $d(\text{V}-\text{O}) = 1.66\text{--}1.68$ Å and $\delta = -550$ ppm. On the basis of these ^{51}V NMR chemical shifts, the $\text{V}-\text{O}$ bond lengths for vanadia-silicalite were estimated to be ca. 1.60 Å for one bond ($\text{V}=\text{O}$) and ca. 1.65 Å for the other three bonds ($\text{V}-\text{O}$).⁴ If this correlation is valid,⁷⁰ the relatively high field chemical shift of **5** can be explained by rather long $\text{V}-\text{O}$ bond lengths, which is consistent with the low stretching frequencies observed for the $\text{V}-\text{O}$ bond and with the position of the O-shells in the XAS radial distribution function.^{4,71} Also, the narrow line width is consistent with a tetrahedral environment that is less distorted than those observed in **3** and **4**.^{4,5}

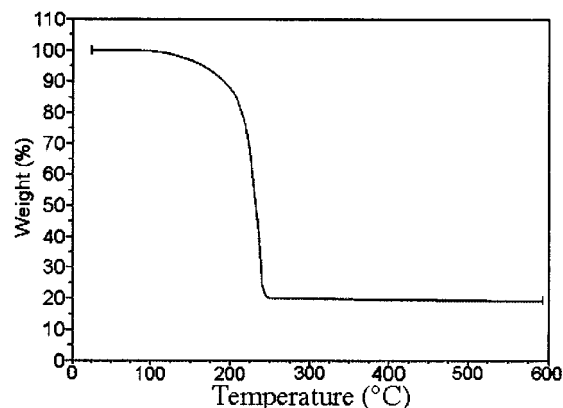
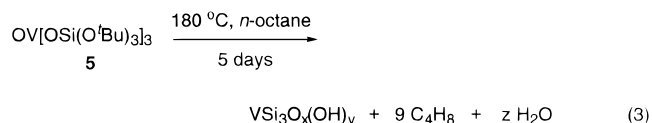


Figure 7. Thermal gravimetric analysis (TGA) trace of **5**.

The ^{29}Si NMR spectrum of **5** contains a broad resonance at -98 ppm ($\omega_{1/2} = 192$ Hz). For comparison, the ^{29}Si NMR resonances for the $\text{Si}-\text{O}-\text{V}$ groups of **3** occur at -63.51 ppm ($\omega_{1/2} = 29$ Hz), and the analogous shifts for the dimer **4** were observed at -64.51 and -64.75 ppm ($\omega_{1/2} = 29$ Hz).²⁶ The ^{29}Si NMR chemical shifts of mesoporous vanadium silicates containing 4-coordinate vanadium(V) were observed at -91 , -101 , and -111 ppm for Q^2 , Q^3 , and Q^4 sites, respectively.¹² The ^{29}Si chemical shift of **5** is therefore very similar (3 ppm to lower field) to that reported for surface sites of type **1a**.

Pyrolytic Conversion of **5 to a V/Si/O Xerogel.** Thermolysis of the vanadyl orthosilicate **5** was first monitored by slow heating in a sealed capillary (under nitrogen) using a melting point apparatus. The opaque white powder melted at $108\text{--}110$ °C, and continued heating at about 3 °C min^{-1} led to the evolution of gas, presumed to be isobutene, at ca. 290 °C. The rate of gas evolution increased rapidly above 300 °C, and at about 310 °C the melt foamed, solidified, and then rapidly turned black, suggesting that **5** melts well below its thermal decomposition temperature. The thermal gravimetric analysis (TGA) curve for **5** (Figure 7) revealed a gradual weight loss between 100 and 200 °C, followed by a dramatic weight loss above 200 °C. The final ceramic yield of 19.4% at 600 °C is considerably less than the theoretical yield (31.7% for $\text{V}_2\text{O}_5 \cdot 6\text{SiO}_2$), but this may be explained by the loss of $(^t\text{BuO})_3\text{SiOH}$ as a volatile elimination product. Indeed, when the thermolysis was carried out on a preparative scale in a tube furnace (under a flow of either O_2 or N_2), considerable amounts of $(^t\text{BuO})_3\text{SiOH}$ were recovered as a sublimate on the cooler walls of the quartz tube. This behavior differs from that of $\text{Zr}[\text{OSi}(\text{O}^t\text{Bu})_3]_4$, which thermally decomposes without melting or subliming.³¹

The thermolysis of **5** in *n*-octane solution was carried out in a flame-sealed, heavy-walled Pyrex tube (eq 3)



in order to inhibit loss of $(^t\text{BuO})_3\text{SiOH}$ in the ceramic conversion. After 5 days of heating at ca. 180 °C, thermolysis resulted in the formation of a dark-green opaque gel. After air-drying for 5 days, the sample was placed under vacuum overnight at 120 °C and then calcined under a flow of oxygen at 500 °C for 3 h. This

(66) Rehr, J. J.; Mustre de Leon, J.; Zabinsky, S. I.; Albers, R. C. *J. Am. Chem. Soc.* **1991**, *113*, 5135.

(67) Mustre de Leon, J.; Rehr, J. J.; Zabinsky, S. I.; Albers, R. C. *Phys. Rev. B* **1991**, *44*, 4146.

(68) Zabinsky, S. I.; Rehr, J. J.; Ankudinov, A.; Albers, R. C.; Eller, M. J. *Phys. Rev. B* **1995**, *52*, 2995.

(69) Rehr, J. J.; Albers, R. C.; Zabinsky, S. I. *Phys. Rev. Lett.* **1992**, *69*, 3397.

(70) Recently the correlation between $\text{V}-\text{O}$ distances and ^{51}V NMR isotropic chemical shifts (δ_{iso}) has been questioned. For further details, see: Skibsted, J.; Jacobsen, C. J. H.; Jakobsen, H. J. *Inorg. Chem.* **1998**, *37*, 3083.

(71) An alternate interpretation for the ^{51}V NMR shift of **5** is based on structural parameters, in particular $\text{V}-\text{O}-\text{Si}$ bond angles.²⁶

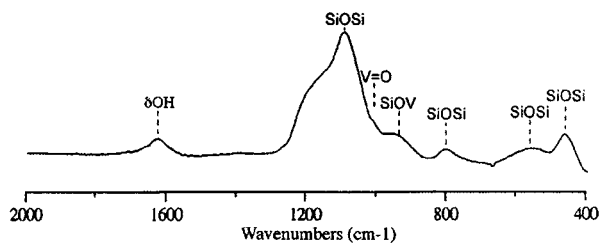


Figure 8. Infrared spectrum of the V/Si/O xerogel.

procedure yielded 0.302 g of the xerogel (from 1.00 g of **5**) as a finely divided, dark-green powder. The ceramic yield is therefore similar to that expected for formation of $V_2O_5 \cdot 6SiO_2$ (31.7%).

The IR spectrum of the V/Si/O xerogel (Figure 8) resembles that of vanadia-substituted silicalite with MFI (ZSM-5) topology.^{5,49} Asymmetric Si–O–Si stretches are observed at 1080 and 1180 (shoulder) cm^{-1} , and lattice vibrations for silica appear at 560 and 450 cm^{-1} .⁵ A small shoulder at 1010 cm^{-1} may be assigned to a V=O vibration, and the band at 940 cm^{-1} appears to correspond to a V–O–Si stretching mode which overlaps with the Si–OH vibration (also see previous discussions of the band assignments for **5**).^{12,14,56–59} A deconvolution of these bands and interpretation of the vanadia dispersion by the method described by Dutoit and Baiker resulted in a Si–O–V/Si–O–Si peak area ratio of 0.12, which may be compared to values of up to 0.11 observed for 10% (w/w) V_2O_5 – SiO_2 aerogels.¹⁴ This suggests a nonoptimal dispersion of vanadium in the case of the V/Si/O xerogel formed from the pyrolysis of **5**.

To establish the nature of the coordination sphere about vanadium, the ligand-to-metal charge-transfer (LMCT) band of the V/Si/O xerogel was studied by DR–UV–vis spectroscopy. The position of the LMCT absorption edge correlates with the vanadium coordination number, as shown by Wokaun et al.¹⁸ For the uncalcined V/Si/O xerogel, an absorption edge at ca. 2.9 eV is consistent with the presence of 5-coordinate vanadium or amorphous V_2O_5 . Upon calcination at 500 °C, the V/Si/O xerogel develops an additional absorption edge at about 2.3 eV, indicating the presence of significant amounts of distorted 6-coordinate vanadium in large domains, as also found in crystalline V_2O_5 . The observed structural rearrangements are probably catalyzed by small amounts of water (a reaction product), which may induce hydrolysis of V–O–V and V–O–Si species and enhance the mobility of vanadia in the composite.^{11,72} Related chemistry was observed for **5**, which reacted with 1 equiv of water in diethyl ether/benzene-*d*₆. No partial hydrolysis products were observed, and V_2O_5 (isolated as a precipitate), $HOSi(O^tBu)_3$, and unhydrolyzed **5** (both identified by ¹H NMR spectroscopy) were the only observed products. This behavior is consistent with the known hydrothermal reactivity of V–O–Si bonds, and with the tendency for hydrated vanadium oxide species to convert readily to V_2O_5 in the presence of silica.^{11,14,29,52,73} In contrast, 4-coordinate vanadia embedded in an ordered silica matrix, as in zeolitic vanadium silicalite, is apparently less sensitive to hydration.^{5,64} Unfortunately, we could not establish

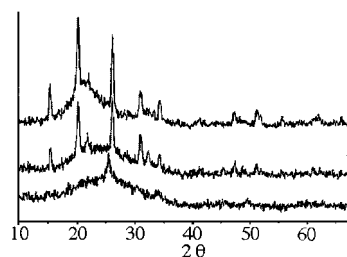


Figure 9. Powder X-ray diffraction patterns of V/Si/O xerogels (a) heated at 120 °C, (b) calcined at 350 °C, and (c) calcined at 750 °C.

the relative amount of 4-coordinate vanadium by DR–UV–vis spectroscopy, as the weak bands expected for this type of center are easily obscured by the more intense lower energy absorption edge for 5-coordinate vanadium: the UV–vis absorption edge for **5** is at 4.2 eV, while those for distorted 5-coordinate/6-coordinate vanadium species typically appear at 2.3–2.9 eV.¹⁸

The vanadium K-edge absorption spectrum was recorded for the $V_2O_5 \cdot 6SiO_2$ xerogel derived from **5** and it was compared to those of NH_4VO_3 and V_2O_5 (see Figure 5).^{60–62} The near-edge normalized X-ray absorption spectrum for this sample looks almost identical to that for V_2O_5 , suggesting similar vanadium centers for both samples.^{60–62} The RDFs of standard vanadium compounds and the xerogel were compared, and it was found that the xerogel RDF resembles that of a mixture of V_2O_5 (major component) and $OV[OSi(O^tBu)_3]_3$ (minor component). This was supported by the fitting of the near-edge EXAFS spectra of the $V_2O_5 \cdot 6SiO_2$ xerogel with a linear combination of the spectra of V_2O_5 and $OV[OSi(O^tBu)_3]_3$, with the predominant species being V_2O_5 . These results are consistent with the vanadium coordination geometry previously proposed from DR–UV–vis spectra.

The calcined V/Si/O xerogel was studied by ²⁹Si MAS NMR spectroscopy in order to determine the dispersion of vanadia in silica. If the local vanadium coordination sphere did not change during ceramic conversion, only Q³ silicon sites would be observed (with isotropic ²⁹Si chemical shift values of ca. –101 ppm).¹² Inhomogeneities in the sample would give rise to Q⁴ sites, with an expected chemical shift of ca. –111 ppm. Deconvolution of the ²⁹Si MAS NMR spectrum into three bands resulted in Q², Q³, and Q⁴ peaks at –94, –101, and –109 ppm, with peak area ratios of 17:48:35, respectively. The presence of the signal at –109 ppm, assigned to Q⁴ sites, indicates that disproportionation of the V–O–Si linkages into V–O–V and Si–O–Si connectivities has occurred during calcination at 500 °C.

Differential thermal analysis (DTA) of the uncalcined, dried V/Si/O xerogel showed exotherms at 368 and 390–400 °C, which likely reflect the crystallization and further phase transitions of V_2O_5 . The melt transition for crystalline V_2O_5 was observed at 672 °C,⁷⁴ and the cooling scan revealed a crystallization exotherm for V_2O_5 at 308 °C. The formation of crystalline V_2O_5 upon calcination of V/Si/O was also confirmed by powder X-ray diffraction, as shown in Figure 9. The powder

(73) Jehng, J. M.; Deo, G.; Weckhuysen, B. M.; Wachs, I. E. *J. Mol. Catal. A* **1996**, *110*, 41.

(74) Sohn, J. R.; Cho, S. C.; Pae, Y. I.; Hayashi, S. *J. Catal.* **1996**, *159*, 170.

(72) Inumaru, K.; Okuhara, T.; Misono, M. *Chem. Lett.* **1990**, 1207.

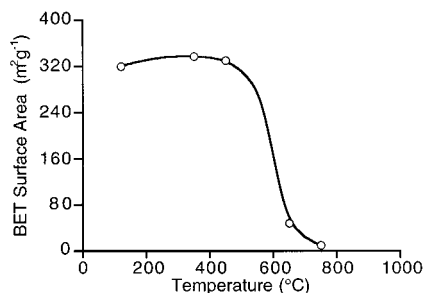
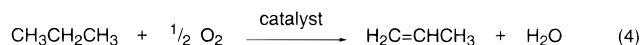


Figure 10. Surface area dependence of the V/Si/O xerogel on calcination temperature.

X-ray pattern of the dried sample (120 °C, vacuum) shows one small broad peak at $2\theta = 25.5^\circ$, corresponding to a d -spacing of 3.49 Å, and a broad halo centered around $2\theta = 25^\circ$. After calcination at 500 °C, peaks corresponding to crystalline V_2O_5 are clearly evident; these peaks sharpen and increase in intensity after the sample is taken to 750 °C.

On the basis of nitrogen BET isotherms for the uncalcined V/Si/O xerogel (type IV with a type H1 hysteresis), the pore structure resembles that of vanadia-silica aerogels.^{13,75} The uncalcined xerogel is mesoporous, having a surface area of 320 m² g⁻¹ and a total pore volume of 2.25 cm³ g⁻¹. The average pore size is 140 Å, but the pore size distribution is bimodal with maxima at about 80 and 200 Å. The dependence of the V/Si/O surface area on the calcination temperature (Figure 10) shows that the xerogel surface area remains constant upon thermal treatment up to about 500 °C (the surface area of the xerogel was 311 m² g⁻¹ after calcination at 500 °C). After calcination at higher temperatures, the material shows a decrease in surface area, and when calcined above the melting point temperature of V_2O_5 (ca. 674 °C),⁷⁴ the material sinters to a surface area of only 8 m² g⁻¹. Note that the surface area we observe is much greater than that reported by Neumann for material obtained by heating "OV[OSi(O'Bu)₃]₃" (generated in solution in the presence of excess HOSi(O'Bu)₃) to ca. 250 °C (25 ± 5 m² g⁻¹).³⁸

Oxidative Dehydrogenation of Propane Catalyzed by the V/Si/O Xerogel. Vanadium silicalite is one of the most efficient catalysts for propane oxidative dehydrogenation (eq 4).¹ In an earlier study we showed



that the cothermolysis of **5** with $\text{Zr}(\text{OCMe}_2\text{Et})_4$ led to active and selective catalysts for the oxidative dehydrogenation (ODH) of propane.³⁷ We also tested the $V_2O_5 \cdot 6\text{SiO}_2$ (34 wt % V_2O_5) xerogel that had been calcined at 500 °C for its catalytic properties.

The propene selectivity as a function of propane conversion is shown in Figure 11. The selectivities and activities for propene formation, extrapolated to 0% propane conversion, were 86.6% and 2.1 mmol g⁻¹ h⁻¹ at 400 °C, 82.1% and 5.6 mmol g⁻¹ h⁻¹ at 450 °C, and 73.2% and 19 mmol g⁻¹ h⁻¹ at 500 °C. The selectivity at 0% conversion provides an intrinsic value containing no contribution from the secondary combustion of pro-

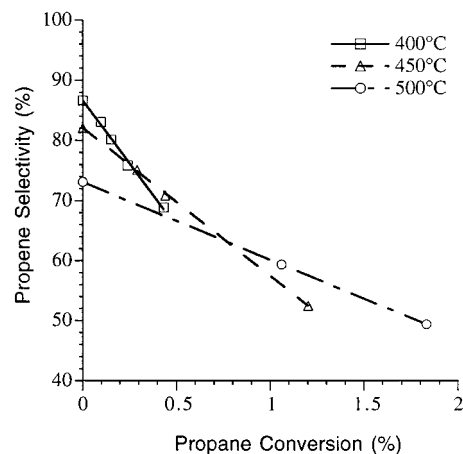


Figure 11. Propane ODH catalysis results for the V/Si/O xerogel catalyst calcined at 500 °C. Reaction conditions: 0.025 g of catalyst, 0.500 g of quartz chips, ambient pressure, feed ratio $\text{O}_2/\text{C}_3\text{H}_8/\text{He}$ of 8:25:200, flow rate range 30–233 mL min⁻¹.

pane, which results in the observed decrease in selectivity with conversion.^{76,77} The activities may also be expressed on the basis of moles of vanadium (rather than grams of catalyst), as 0.16 mmol (mol V)⁻¹ s⁻¹ at 400 °C, 0.42 mmol (mol V)⁻¹ s⁻¹ at 450 °C, and 1.4 mmol (mol V)⁻¹ s⁻¹ at 500 °C. Extrapolating these values to 333 °C ($E_a = 93$ kJ mol⁻¹), we obtain a rate of 0.025 mmol (mol V)⁻¹ s⁻¹ at this temperature, and this allows us to compare our catalyst to other systems. An analogous system with 15 wt % V_2O_5 , prepared by the incipient wetness impregnation of ammonium metavanadate onto silica, exhibited a lower selectivity and a similar activity [67% and 0.031 mmol (mol V)⁻¹ s⁻¹, under similar reaction conditions].⁷⁶ Furthermore, the latter catalyst has a lower surface area (251 m² g⁻¹) after being treated under an identical temperature regime and clearly contains V_2O_5 crystallites (by XRD and DR-UV-vis and Raman spectroscopy).⁷⁷ This suggests that our procedure for preparing catalysts may have advantages over more traditional, impregnation methods. The $V_2O_5 \cdot 6\text{SiO}_2$ xerogel is also similar to bulk V_2O_5 in its ODH of propane (which exhibits a selectivity of about 80%, with a catalyst surface area of 3 m² g⁻¹) and rapidly declining selectivity with increasing conversions.^{3,77}

Conclusion

The binary vanadia-silica precursor **5** provides a good model for isolated vanadia on silica and avoids the problems associated with carbon-containing ligands in previous model complexes **2–4**. Characterization data for **5** provides a firmer basis for the spectroscopic characterization of isolated vanadyl sites on silica. For example, Raman spectroscopy allowed assignment of the O=V vibration at 1038 cm⁻¹ and clearly revealed a band that can be assigned to the symmetric V–O stretch (at 651 cm⁻¹). These frequencies allow estimation of the V=O and V–O bond lengths for **5**, which were in good agreement with the values obtained from XAS studies.

(75) Sing, K. S. W.; Everett, D. H.; Haul, R. A. W.; Moscou, L.; Pierotti, R. A.; Rouqu erol, J.; Siemieni ska, T. *Pure Appl. Chem.* **1985**, *57*, 603.

(76) Khodakov, A.; Olthof, B.; Bell, A. T.; Iglesia, E. *J. Catal.* **1999**, *181*, 205.

(77) Khodakov, A.; Yang, J.; Su, S.; Iglesia, E.; Bell, A. T. *J. Catal.* **1998**, *177*, 343.

The IR spectrum for **5** indicates that two bands of equal intensity exist for the stretching frequencies of Si–O–V and that IR bands attributed to the V=O and V–O bonds are relatively weak.

Thermolysis of **5** forms water, which catalyzes V–O–Si cleavage and the formation of V–O–V bonds. As a result, the new material formed from **5** (after calcination at 500 °C) does not consist of isolated 4-coordinate vanadium in a matrix of silica as in **5**, but mainly of 5-coordinate V₂O₅ and silica as shown by DR–UV–vis and ²⁹Si NMR spectroscopies, XAS, and powder X-ray diffraction. Thus in this case, the single-source precursor does not appear to give a highly dispersed mixed-element sample. This might be an artifact of the high vanadium loading, and dilution by other precursor species might be highly beneficial in this regard. Previous work showed that if metal alkoxides are added to the heated solution of **5**, water is removed in situ and highly dispersed ternary metal oxides, which are good catalysts for oxidative dehydrogenation of propane, can be obtained from the precursor **5**.^{36,37} Future work will focus on the production of ternary V/Si/M/O xerogels via a thermolysis–hydrolysis procedure using **5** and metal alkoxides.

Experimental Section

General. DR–UV–vis measurements (Cary 4 UV–Visible spectrophotometer from Varian) were performed on powder films with MgO as a background reference for the V/Si/O xerogel and in transmittance mode on hexane solutions of **5**. Raman spectra (Hololab series 5000 from Kaiser Optical Systems Inc.) were recorded with samples (in powdered or liquid form) encased in glass capillaries, using a laser (60 mW, 532 nm). FT-IR (Mattson Infinity Series FTIR) was performed in transmission mode on hexane solutions of HOSi(O^tBu)₃ and **5** and as a KBr pellet for the V/Si/O xerogel. Solution ¹H and ¹³C NMR spectra were measured with an AMX 300 MHz NMR spectrometer from Bruker. Solution ⁵¹V and ²⁹Si NMR spectra were obtained with a DRX 500 Bruker NMR spectrometer. ²⁹Si MAS NMR spectra were measured on a 400 MHz Varian solid-state spectrometer at an operating frequency of 79.48 MHz and were carried out by Dr. Tim Burrow at the University of Toronto. Nitrogen BET surface area analysis was performed on an Autosorb 6 from Quantachrome. Combustion analyses and mass spectrometry were carried out in the College of Chemistry's Microanalytical Facility at the University of California, Berkeley. All manipulations were carried out with dried solvents under an atmosphere of nitrogen using Schlenk line techniques or an inert glovebox, unless indicated otherwise.

X-ray absorption measurements were carried out at Stanford Synchrotron Radiation Laboratory (SSRL) using beamline 2–3. X-ray detection was performed in the transmission mode using two ion chambers and a double crystal (Si111) monochromator at the K-edge of vanadium (5463 eV). X-ray absorption data for the vanadium catalysts and standard compounds (distorted square pyramidal V₂O₅ and tetrahedral NH₄VO₃)^{61,62} were analyzed using WinXas 97 (v 1.1) software.^{78,79} The inflection point in the K-edge was taken as the edge energy. The pre-edge region of the spectrum was fitted by a straight line and extrapolated to the edge energy. In the post-edge region, a polynomial spline fit to the nonoscillatory component of the spectrum was extrapolated to the edge energy. The difference between the two extrapolated values is a measure

of the increase in absorption characteristic of the K-edge and is commonly known as the absorption jump. The complete spectrum was normalized to this quantity.^{60,65,80,81}

Catalysis. Selectivities and conversion measurements were carried out in a fixed-bed quartz reactor using 0.025 g of catalyst mixed with 0.500 g of quartz chips. The reactions were carried out under ambient pressure with a feed ratio O₂/C₃H₈/He of 8:25:200. Propane conversion was varied by manipulating the flow rate between 30 and 233 mL min⁻¹. The C₃H₈ and O₂ conversions were below 4 and 10%, respectively.

Online analysis of reactants and products was performed using a Hewlett-Packard 5880 gas chromatograph equipped with a carboxen column. Only C₃H₆, H₂O, CO, and CO₂ were detected as reaction products.

OV[OSi(O^tBu)₃]₃ (5**).** At room temperature, 1.156 g of OVCl₃ (6.7 mmol) was added rapidly to a vigorously stirred solution of 1.7 mL of pyridine (21 mmol) and 5.28 g (20 mmol) of HOSi(O^tBu)₃ in 75 mL of benzene. Stirring was continued for 24 h, after which the pyridinium hydrochloride was separated by filtration and washed with 50 mL of hexanes. After removal of the volatile material from the combined filtrate and extracts, the resulting solid was dried under vacuum for 2 h to give the product in 92% yield (5.25 g) as a white crystalline powder. The compound thus isolated may contain small amounts of HOSi(O^tBu)₃ as an impurity. Further purification was accomplished by recrystallization from 20 mL of CH₂Cl₂ at –40 °C, to give 4.85 g of analytically pure OV[OSi(O^tBu)₃]₃ (85%): mp 108–110 °C; Anal. Calcd for C₃₆H₈₁O₁₃–SiV: C, 50.44; H, 9.52. Found: C, 50.58; H, 9.59. ¹H NMR (300 MHz, benzene-*d*₆) δ 1.51 (s); ¹³C NMR (75.5 MHz, benzene-*d*₆) δ 31.89, 73.35; ²⁹Si NMR (99.35 MHz, benzene-*d*₆) δ –98; ⁵¹V NMR (105 MHz, benzene-*d*₆) δ –777; UV–vis (hexane) 250 nm, ε 9.8 × 10³ M⁻¹ cm⁻¹; IR (hexane, CsI) 1388 w, 1366 m, 1243 m, 1191 m, 1073 vs, 1029 w sh, 1010 w sh, 920 s, 910 s, 833 w, 810 vw, 705 w, 672 vw, 502 w sh, 477 m cm⁻¹; Raman (solid) 2979 vs, 2928 vs, 2780 w, 2714 m, 1451 s, 1367 vw, 1244 m, 1190 w, 1066 w sh, 1038 s, 1010 w sh, 914 s, 834 w, 808 s, 705 w sh, 674 w sh, 651 m, 545 s, 465 m, 433 vw, 370 w, 337 vw, 260 w, 231 w, 183 w cm⁻¹; MS (EI, 40 eV) 991 (V[OSi(O^tBu)₃]₄ – 2 CH₂C(CH₃)₂), 935 (V[OSi(O^tBu)₃]₄ – 3 CH₂C(CH₃)₂), 857 (HOV[OSi(O^tBu)₃]₃), 841 (HV[OSi(O^tBu)₃]₃).

V/Si/O Xerogel. Inside a glovebox, a thick-walled 100 mL Pyrex tube with a narrow neck, fitted with a stopcock, was charged with 1.00 g of **5** and 8 mL of *n*-octane. The solution was subjected to two freeze–pump–thaw cycles and the tube was sealed with a flame. The complete tube with its contents was placed in an oven heated to 180 °C. After 4 days a green-black opaque gel had formed. After heating an additional 24 h, the tube and its contents were cooled to room temperature. The octane solvent was allowed to evaporate in air over 5 days, and the resulting deep green solid powder was dried under vacuum at 120 °C for 15 h. The sample was then calcined under an atmosphere of oxygen at 500 °C for 3 h. Thus 0.302 g of V/Si/O was isolated (95% yield, assuming the formation of V₂Si₆O₁₇). Measurements and catalysis were performed with the calcined material unless stated otherwise.

Acknowledgment. This work was supported by the Director, Office of Energy Research, Office of Basic Energy Sciences, Chemical Sciences Division, of the U.S. Department of Energy under Contract No. DE-AC03-76SF00098. X-ray absorption experiments were performed at the Stanford Synchrotron Radiation Laboratory (SSRL) and supported, in part, by the U.S. Department of Energy. We thank Dr. George D. Meitzner for helpful discussions.

CM9903500

(78) Ressler, T. J. *de Physique IV* **1997**, 7, 269.

(79) Ressler, T. J. *Synch. Rad.* **1998**, 5, 118.

(80) Meitzner, G.; Via, G. H.; Lytle, F. W.; Sinfelt, J. H. *J. Phys. Chem.* **1992**, 96, 4960.

(81) Sinfelt, J. H.; Meitzner, G. D. *Acc. Chem. Res.* **1993**, 26, 1.